SETSCI Conference Indexing System,
Volume 3 (2018), 66-71

ISAS 2018-Winter
2nd International Symposium on Innovative Approaches in Scientific Studies
November 30 – December 2, 2018, Samsun, Turkey

Thermal Characteristics of Swirling Coaxial Confined Impinging Air Jets: An Experimental Investigation

Burak Markal[1*+]

Department of Energy Systems Engineering, Recep Tayyip Erdogan University, 53100 Rize, Turkey
**Corresponding author: burak.markal@erdogan.edu.tr*
+Speaker: burak.markal@erdogan.edu.tr
Presentation/Paper Type: Oral / Full Paper

Abstract – The present study investigates the heat transfer characteristics of swirling coaxial confined impinging turbulent air jets. Experimental range covers different values of dimensionless nozzle-to-plate distance (H / D = 0.5, 1 and 2) and dimensionless flowrate ratio (Q* = 0.2 and 0.5). The total flowrate is kept constant at 1.16 x 10^{-3} m^3 s^{-1} (70 L/min) during the tests. The results are also compared to those obtained for the conventional single circular jets (Q* = 0). It is concluded that both the intensity and the radial uniformity of the heat transfer are improved by increasing dimensionless flowrate ratio. On the other hand, increasing nozzle-to-plate distance causes a decrement in the magnitude of Nusselt numbers.

Keywords – *Impingement, swirling jet, coaxial, heat transfer, radial uniformity*

I. INTRODUCTION

Effective thermal management is very important for longevity of the systems and/or system components work under high thermal loads. In this regard, impinging jet is one of the most promising methods to remove higher amount of heat from the surfaces. It should be noted that impinging jets are also used for heating and mass transfer applications in addition to cooling processes. Thus, this method has a very large usage area such as tempering and shaping of glass, drying of textiles and paper [1], cooling of electronic components [2] and gas turbine blades [3], etc. Due to the high heat and mass transfer performance, lots of researchers focus on the studies dealing with jet flows.

In the simplest form, a conventional single circular or slot impinging jet consists of three main flow regions: (1) free jet region, (2) impingement region and (3) wall jet region [4]. Flow behavior in these regions closely depend on many geometrical and flow characteristics such as fluid type, nozzle geometry, impingement surface roughness, flow exit angle (oblique outlets), nozzle-to-plate distance, Reynolds number, etc. Different ranges of the mentioned parameters and their combined effect can lead to different results. Therefore, the subject is open to improvement and there are lots of studies in the literature.

Maki and Yabe [5] studied annular impinging jet ejected from an annular nozzle. They concluded that the Nusselt number at the reverse stagnation point had a weak dependency on the Reynolds number. Huang and El-Genk [6] researched and compared the performances of swirling and conventional multi-channel impinging jets through heat transfer and flow visualization tests. They concluded that swirling impinging jets led to higher Nusselt numbers and obvious enhancements in radial uniformity in heat transfer compared to the multi-channel and conventional ones. Can and Etemoglu [7] examined two methods for enhancing heat transfer under impinging air jets: (1) by artificially raising the turbulence level, and (2) by acoustic excitement of the jet. For both of the cases, they obtained modest enhancement in heat transfer. Nuntadusit et al. [8] experimentally focused on the flow and heat transfer characteristics of multiple swirling impinging jets for different jet to jet distances for a constant nozzle-to-plate distance of 4. They used twisted tapes for introducing swirling motion. They declared that the multiple swirling impinging jets showed higher heat transfer than the multiple conventional jets. Eiamsa-ard et al. [4] conducted an experimental study for the heat transfer behavior of co/counter-dual swirling impinging jet arrangements. They placed two twisted-tapes into a pipe as a swirl generator. They concluded that for small nozzle-to-plate distances swirling jets were advantageous in terms of heat transfer compared to the conventional ones. Wae-Hayee et al. [9] numerically and experimentally investigated in-line impinging jets in cross-flow for short nozzle-to-plate distances. They concluded that the peak value of the Nusselt number increased with increasing cross-flow velocity. Ahmed et al. [10, 11] focused on flow and heat transfer characteristics of swirling and non-swirling turbulent impinging jets. They stated that at lower impingement distances the swirling jet presented higher heat transfer performance. Markal [12] experimentally studied heat transfer characteristics and wall pressure distribution of swirling coaxial confined impinging air jets. It was concluded that increasing flowrate ratio improved both the radial uniformity and intensity of heat transfer. Markal and Aydin [13] experimentally investigated hydrodynamical and thermal characteristics of coaxial confined impinging turbulent air jets. They underlined the importance of the dimensionless flowrate ratio, and also stated that increasing nozzle-to-plate distance decreased the intensity of heat transfer.

Some studies related to the impinging jets are summarized above. In the literature, the experimental investigation of the swirling coaxial confined impinging air jets has been conducted firstly by Markal [12]. However, as it is stated above, the flow structures, and thus, the heat transfer

characteristics are closely related to the experimental conditions. Therefore, new studies should be performed under different experimental conditions for further understanding of the subject. Thus, the aim of the present study is to investigate the effects of dimensionless nozzle-to-plate distance and dimensionless flowrate ratio on the heat transfer characteristics of swirling coaxial confined impinging air jets. In this regard, local Nusselt number distributions and area-averaged Nusselt numbers are obtained for different test cases. Also, the results obtained for coaxial cases are compared to the conventional single circular jet results.

II. Materials and Method

Figure 1 presents the schematic diagram of the experimental setup. All the equipments are numbered and defined in the relevant figure. The setup and working principle can be shortly described as follows: The atmospheric air in the laboratory is compressed and sent to the air tank. The working fluid (air) used in the experiments is supplied from the air tank. During this process, firstly, the air passes through a filter and a dryer unit. Then, the flow line is separated into two lines. There are a pressure regulator, a valve and a rotameter in each line. The flowrate in each flow passage of the nozzle (inner circular and outer swirl flow passages) can be easily adjusted via these equipments. One of the experimental parameters is the nozzle-to-plate distance which is adjusted by a movement mechanism moves in the vertical direction. The jet flow ejected from the nozzle impinged onto the impingement plate. The impingement plate is heated via a flexible heater connected to a power supply. Temperature values are measured via micro thermocouples related to the data logger. Experiments have been performed at steady state conditions.

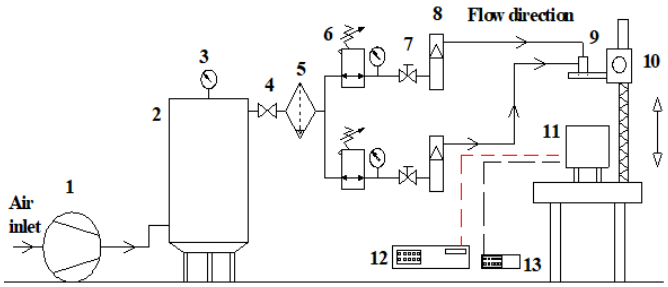

Fig. 1 The schematic diagram of the experimental setup

Figure 2 shows the solid pictures of the nozzle. The brass nozzle is put into a Delrin holder. Figure 2a presents the sectional view of the assembly. The nozzle is a coaxial type one and involves an inner circular (round) flow passage with the diameter of 4.5 mm and three outer helical passages (machined symmetrically, with 120º). The width (w_s) and the height (h_s) of each helical passage are 2 mm and 1.5 mm, respectively (see Fig. 2b). The outer diameter (D) and the length of the nozzle are 10 mm and 29 mm, respectively. The swirl angle and the swirl number are 45º and 0.86, respectively. The outer diameter of the Delrin holder is 30 mm.

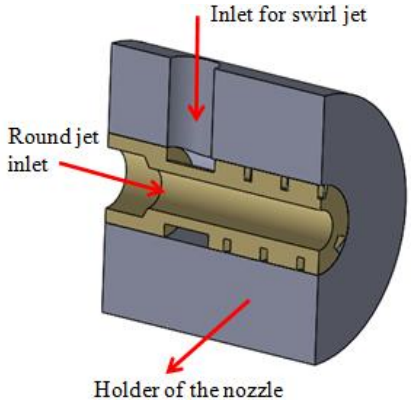

(a)

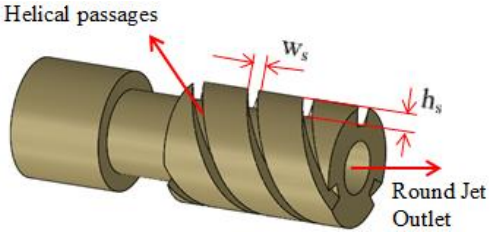

(b)

Fig. 2 Solid pictures of the nozzle used in the experiments

Detailed view of the copper impingement plate is presented in Fig. 3. Its diameter and thickness are 46 mm and 1.5 mm, respectively. However, a section at the backside of the plate is grooved, and here, the thickness is reduced to 0.2 mm for more accurate temperature readings. The micro thermocouples are glued on the wall of this groove. The thermocouples are placed with 3 mm spacing. The gap is filled with a thermally conductive paste, and beneath the impingement plate, a flexible heater is placed. Glass wool is used for thermal insulation of the test section. During the experiments, the temperature of the air in the laboratory is kept constant at approximately 22 ºC and a constant heating power of 18.2 W is applied via flexible heater.

An uncertainty analysis is performed based on the procedure defined by Kline and McClintock [14], and the relevant uncertainties are presented in Table 1. The details related to the experimental setup, uncertainty analysis, devices, test section and test procedures are presented in the recent article of the author [12].

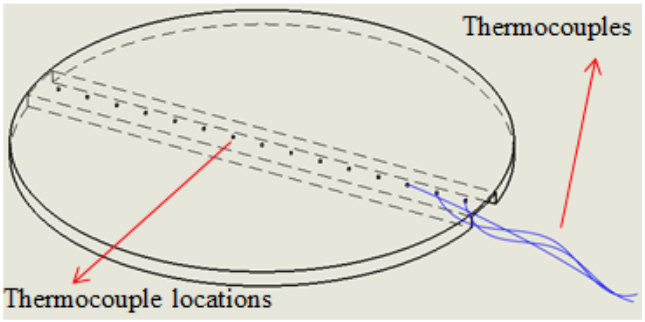

Fig. 3 Detailed view of the copper impingement plate

Table 1 Experimental uncertainties

Measurements and Derived Parameters	**Uncertainty (Maximum values for derived parameters)**
Temperature, T	±0.1 ºC
Flow rate, Q	±3 %
Applied power, q	±0.1 %
Reynolds number, Re	±4.2 %
Nusselt number, Nu	±5.0 %

The local convective heat transfer coefficient and the local and area-averaged Nusselt numbers are presented as follows, respectively:

$$h = \frac{q_{conv}}{A_s (T_s - T_j)} \quad (1)$$

$$Nu = \frac{hD}{k} \quad (2)$$

$$Nu_{avg} = \frac{\bar{h}D}{k} \quad (3)$$

where, q_{conv} is the heat loss due to the convection, A_s is the surface area of the impingement plate, T_s is the surface temperature, T_j is the jet temperature, $\bar{h}$ is the area-weighted average heat transfer coefficient, D is the outer diameter of the nozzle and k is the thermal conductivity. In the calculations, conduction and radiation heat losses are subtracted from the applied heating power to obtain the convection heat loss.

The dimensionless flowrate ratio refers to the volumetric flowrate in the swirling passages over the total volumetric flowrate, and it is represented as follows:

$$Q^* = \frac{Q_s}{Q_{tot}} \quad (4)$$

$$Q_{tot} = Q_s + Q_r \quad (5)$$

Here, Q is the volumetric flowrate, and the subscripts of *tot*, *r* and *s* represent total, round and swirl (all the swirling channels), respectively. One of the research parameters is the dimensionless nozzle-to-plate distance defined as H / D where H is the distance between the nozzle exit and the impingement surface. The dimensionless radial distance is defined as below:

$$r^* = \frac{r}{D} \quad (6)$$

where, r is the radial distance measured from the stagnation point. The details related to the data reduction can be found in Markal [12].

III. Results and Discussion

In this paper, experiments are conducted for different values of dimensionless nozzle-to-plate distance (H / D = 0.5, 1 and 2) and dimensionless flowrate ratio (Q^* = 0.2 and 0.5) at a constant total flowrate of 1.16 x 10^{-3} m^3 s^{-1} (70 L/min). The flow is incompressible (Mach number < 0.3).

Figures 4a and b show the variation of the local Nusselt numbers with the dimensionless radial distance as a function of dimensionless nozzle-to-plate distance for different dimensionless flowrate ratio. Due to the symmetry with respect to the origin, half of the graphs are given. For both of the flowrate ratio values, it is clearly seen that increasing distance between the jet exit and the impingement plate negatively effects the magnitudes of the Nusselt numbers over all the radial direction. This result can be attributed to the decreasing influence of the axial flow, and hence, reducing of the kinetic energy. Increasing impingement distance causes jet spreading, and the jet spreading leads to the weakening of the axial flow [4, 15]. Also, it can be added that, as a result of increasing nozzle-to-plate distance thermal boundary layer gets thicker, temperature gradient decreases, and thus, the intensity of the convective heat transfer decreases. Towards the outer edges of the impingement plate, this decrement is more obvious due to the thicker boundary layers.

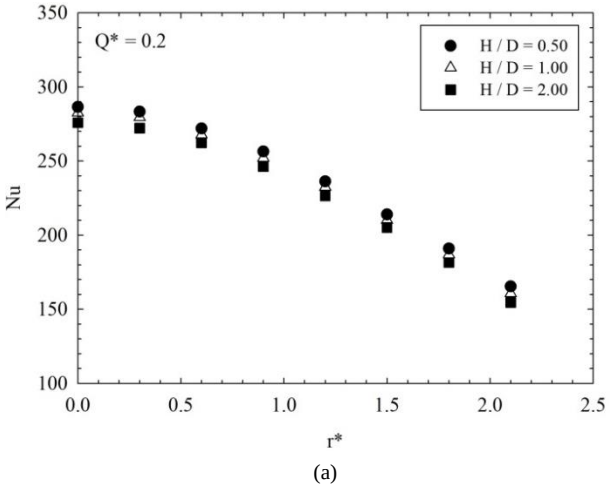

(a)

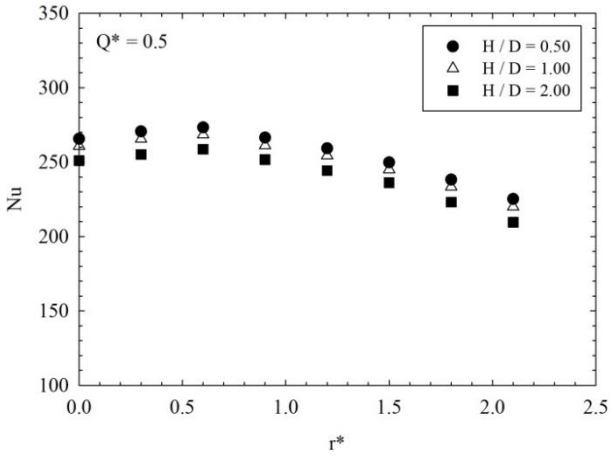

(b)

Fig. 4 Variation of the local Nusselt numbers with the dimensionless radial distance as a function of dimensionless nozzle-to-plate distance for different dimensionless flowrate ratio

Figures 5a, b and c present variation of the local Nusselt numbers with the dimensionless radial distance as a function of dimensionless flowrate ratio for different dimensionless nozzle-to-plate distances. As it is clearly seen from the graphs, for all the spacing, the uniformity of heat transfer is obviously enhanced by increasing dimensionless flowrate ratio. The reason of this result can be explained with the mixing of the flow and formation of the vortices in the flow field. In the present paper, increasing flowrate ratio means increasing contribution of the swirling flow. The swirling flow has some merits compared to the conventional circular flow. Most important characteristic of the swirling flow compared to the conventional circular flow (for impinging jets) is its tangential velocity component. The existence of tangential components enhances the mixing and extends the impact areas of the jet flow, which makes the thermal boundary layer thinner, and hence, increases the thermal performance. As a result, increasing dimensionless flowrate ratio enhances the mixing of the flows and causes vortices which improve the turbulence characteristics. In the literature, it is stated that higher air mass flux on the perimeter region of the jet flow field improves turbulence in the stagnation region [6], and increasing flowrate value can lead the stagnation region to spread radially outward. It should be noted that increasing dimensionless flowrate ratio means increasing mass flux in radially outward regions. Of course, the swirling characteristic of the outer jet has very important role on the radial spreading.

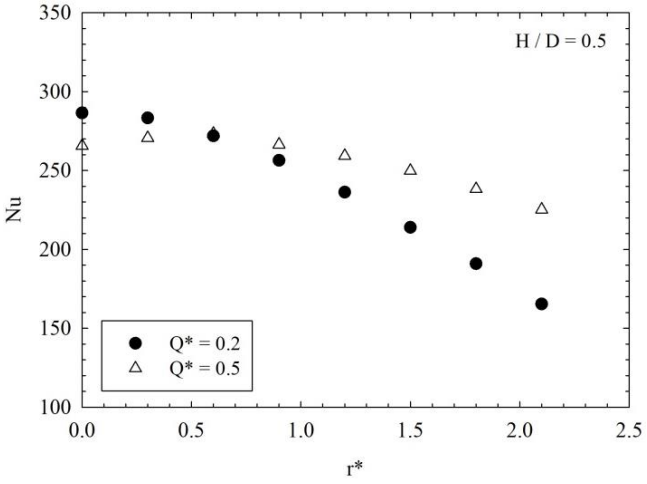

(a)

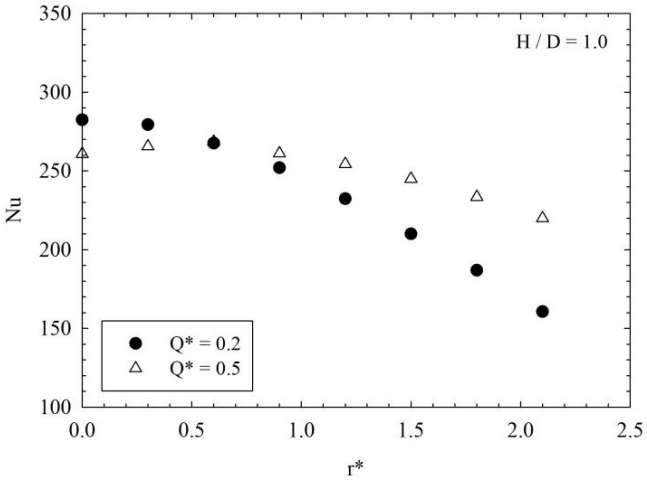

(b)

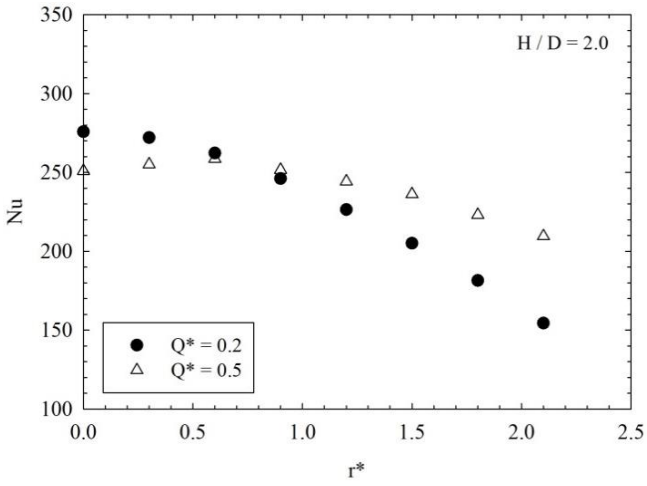

(c)

Fig. 5 Variation of the local Nusselt numbers with the dimensionless radial distance as a function of dimensionless flowrate ratio for different nozzle-to-plate distances

Significant enhancements in heat transfer, especially towards the radially outward regions, improve the area-weighted average Nusselt numbers due to the larger heat transfer areas. For a quantitative analysis, the values of the averaged Nusselt number and stagnation Nusselt numbers for experimental conditions are presented in Table 2 and 3, respectively. As it is seen from Table 2, averaged Nusselt number obviously increases with increasing dimensionless flowrate ratio (up to 19.6%) and decreasing nozzle-to-plate distance (up to 6%). On the contrary, the stagnation Nusselt number decreases with increasing flowrate ratio (up to 9%). In the cases with higher flowrate ratio, the flowrate of the inner circular jet is less. Therefore, the momentum of the central circular jet decreases, which causes a reduction in the stagnation point Nusselt number value.

Table 2 The values of averaged Nusselt number

	$\mathbf{Nu_{avg}}$	
	Q* = 0.2	**Q* = 0.5**
H / D = 0.5	204.50	243.82
H / D = 1.0	199.50	238.71
H / D = 2.0	194.02	229.18

Table 3 The values of stagnation Nusselt number

	Nu_{st}	
	Q* = 0.2	**Q* = 0.5**
H / D = 0.5	286.54	265.74
H / D = 1.0	282.54	260.82
H / D = 2.0	275.91	250.97

Figure 6 shows the comparison of the swirling coaxial jet with the conventional circular jet based on surface temperature distribution. As it is seen from Fig. 6, there is a significant reduction in the temperature values towards the outer edges of the impingement plate by increasing flowrate ratio. This reduction leads to enhancement of the heat transfer as it is stated and explained above in detail. Also, for conventional jet ($Q^* = 0$) the temperature values in the stagnation point and its vicinity are lower than those of the coaxial case due to the higher kinetic energy.

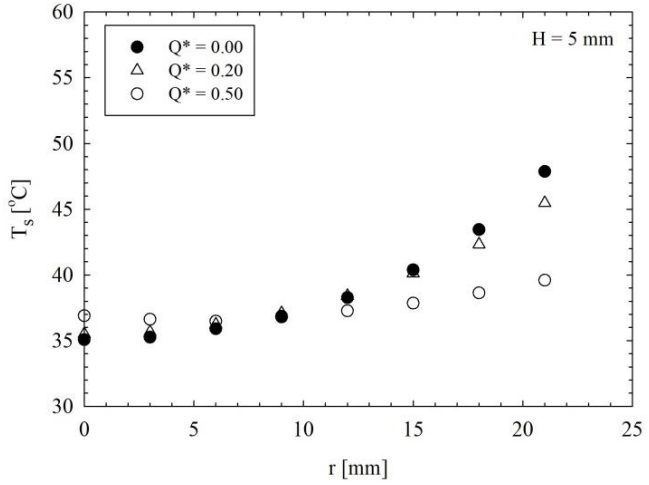

(a)

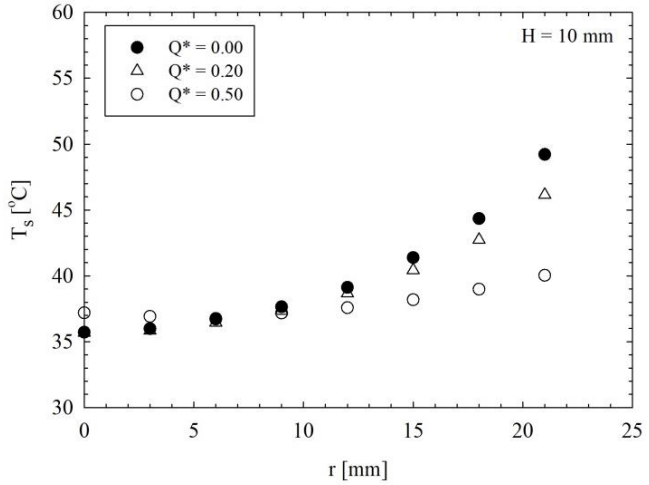

(b)

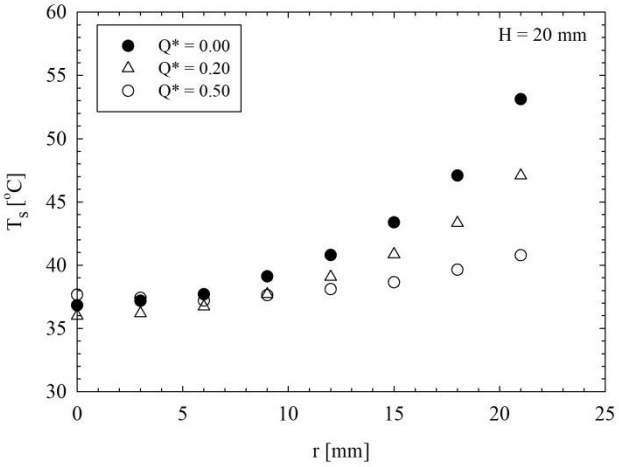

(c)

Fig. 6 Comparison of the swirling coaxial jet with the conventional circular jet based on surface temperature distribution

IV. CONCLUSION

In the present study, heat transfer characteristics of swirling coaxial confined impinging turbulent air jets are experimentally investigated. The main conclusions can be summarized as follows:

- Increasing distance between the jet exit and the impingement plate negatively affects the magnitudes of the Nusselt numbers over all the radial direction.
- The uniformity of heat transfer is obviously enhanced by increasing dimensionless flowrate ratio.
- Averaged Nusselt number increases with increasing dimensionless flowrate ratio (up to 19.6%) and decreasing nozzle-to-plate distance (up to 6%).
- The stagnation Nusselt number decreases with increasing flowrate ratio (up to 9%).
- There is a significant reduction in the temperature values towards the outer edges of the impingement plate by increasing flowrate ratio. However, for conventional jet ($Q^* = 0$) the temperature values in the stagnation point and its vicinity are lower than those of the coaxial case.

REFERENCES

[1] D. W. Colucci, and R. Viskanta, "Effect of nozzle geometry on local convective heat transfer to a confined impinging air jet," *Exp. Therm Fluid Sci.*, vol. 13, pp. 71−80, 1996.

[2] X. Gao, and B. Sunden, "Experimental investigation of the heat transfer characteristics of confined impinging slot jets," *Exp. Heat Transf.*, 16, pp. 1–18, 2003.

[3] M. F. Koseoglu, and S. Baskaya, "The effect of flow field and turbulence on heat transfer characteristics of confined circular and elliptic impinging jets," *Int. J. Therm Sci.*, vol. 47, pp. 1332–1346, 2008.

[4] S. Eiamsa-ard, K. Nanan, and K. Wongcharee, "Heat transfer visualization of co/counter-dual swirling impinging jets by thermochromic liquid crystal method," *Int. J. Heat Mass Transf.*, vol. 86, pp. 600–621, 2015.

[5] H. Maki, and A. Yabe, "Heat transfer by the annular impinging jet, *Exp. Heat Transf.*, vol. 2:1, pp. 1−12, 1989.

[6] L. Huang, and M. S. EL-Genk, "Heat transfer and flow visualization experiments of swirling, multi-channel, and conventional impinging jets," *Int. J. Heat Mass Transf.*, vol. 41, pp. 583–600, 1998.

[7] M. Can, and A. B. Etemoglu, "Investigation into methods of enhancing heat transfer under impinging air jets," *Exp. Heat Transf.*, vol. 16:3, pp. 171−190, 2003.
[8] C. Nuntadusit, M. Wae-hayee, A. Bunyajitradulya, and S. Eiamsa-ard, "Visualization of flow and heat transfer characteristics for swirling impinging jet," *Int. Commun. Heat Mass Transf.*, vol. 39, pp. 640–648, 2012.
[9] M. Wae-Hayee, P. Tekasakul, S. Eiamsa-ard, and C. Nuntadusit, "Flow and heat transfer characteristics of in-line impinging jets with cross-flow at short jet-to-plate distance, *Exp. Heat Transf.*, vol. 28:6, pp. 511−530, 2015.
[10] Z. U. Ahmed, Y. M. Al-Abdeli, and F. G. Guzzomi, "Heat transfer characteristics of swirling and non-swirling impinging turbulent jets," *Int. J. Heat Mass Transf.*, vol. 102, pp. 991–1003, 2016.
[11] Z. U. Ahmed, Y. M. Al-Abdeli, and F. G. Guzzomi, "Flow field and thermal behaviour in swirling and non-swirling turbulent impinging jets," *Int. J. Therm. Sci.*, vol. 114, pp. 241–256, 2017.
[12] B. Markal, "Experimental investigation of heat transfer characteristics and wall pressure distribution of swirling coaxial confined impinging air jets," *Int. J. Heat Mass Transf.*, vol. 124, pp. 517–532, 2018.
[13] B. Markal, and O. Aydin, "Experimental investigation of coaxial impinging air jets," *Appl. Therm. Eng.*, vol. 141, pp. 1120–1130, 2018.
[14] S. J. Kline, and F. A. McClintock, "Describing uncertainties in single-sample experiments," *Mech. Eng.*, vol. 75 (1), pp. 3–8, 1953.
[15] Y. Ozmen, "Confined impinging twin air jets at high Reynolds numbers," *Exp. Therm Fluid Sci*., vol. 35, pp. 355–363, 2011.